

Revisiting the $R\nu$ MDM Models

Yi Cai^{*1} and Michael A. Schmidt^{†2}

¹ARC Centre of Excellence for Particle Physics at the Terascale, School of Physics, The University of Melbourne, Victoria 3010, Australia

²ARC Centre of Excellence for Particle Physics at the Terascale, School of Physics, The University of Sydney, NSW 2006, Australia

Abstract

Combining neutrino mass generation and a dark matter candidate in a unified model has always been intriguing. We revisit the class of $R\nu$ MDM models, which incorporate minimal dark matter in radiative neutrino mass models based on the one-loop ultraviolet completions of the Weinberg operator. The possibility of an exact accidental Z_2 is completely ruled out in this scenario. We study the phenomenology of one of the models with an approximate Z_2 symmetry. In addition to the Standard Model particles, it contains two real scalar quintuplets, one vector-like quadruplet fermion and a fermionic quintuplet. The neutral component of the fermionic quintuplet serves as a good dark matter candidate which can be tested by the future direct and indirect detection experiments. The constraints from flavor physics and electroweak-scale naturalness are also discussed.

1 Introduction

The particle identity of dark matter is one of the most important problems in physics beyond the Standard Model (SM). Generally in dark matter models a discrete symmetry, Z_2 symmetry as the simplest example, has to be imposed by hand or show up as the remnant symmetry of a larger group to protect the dark matter particle from decaying. Alternatively, the SM gauge group can be used to stabilize dark matter as discussed in minimal dark matter (MDM) [1; 2] models. Higher representations of $SU(2)_L$ are introduced in MDM models as dark matter candidates. They couple to the SM sector only through gauge interactions, while other types of interactions such as Yukawa interactions or scalar interactions are all forbidden by $SU(2)_L$ due to their large dimensions¹. As a result, an *accidental* (approximate) Z_2 symmetry is present. The symmetry might be exact or approximately realised if the lifetime is larger than the age of the Universe.

If we consider more than just a single $SU(2)_L$ multiplet, we might be able to write down an interaction between SM fermions or Higgs and a pair of dark sector particles. It is of great interests to see whether it is possible to simultaneously explain the origin of neutrino masses and mixings, another clear evidence for physics beyond the SM. There is a rich literature on dark matter in neutrino mass models (See Refs. [4–9] for example.). The usual seesaw mechanisms [10–21] obviously can not be incorporated in the framework of MDM, as the intermediate particles couple to a pair of SM particles and thus are even under the accidental Z_2 of MDM. Therefore

^{*}yi.cai@unimelb.edu.au

[†]michael.schmidt@sydney.edu.au

¹Higher dimensional operators, which might be present, can still lead to dark matter decay. See Ref. [3] for a recent discussion.

we turn our eyes to the next-to-minimal solution, radiative neutrino mass generation [22]. We will focus on minimal ultraviolet (UV) completions of the Weinberg operator.

This idea of realizing radiative neutrino mass in a minimal dark matter model, coined as $R\nu$ MDM, was proposed in Ref. [23], where a scalar sextet and a fermionic quintuplet are introduced. The neutrino mass would be generated at one-loop level. However, the accidental Z_2 symmetry is broken by a quartic coupling of three scalar multiplets with one Higgs [24] and it can be only approximately realised in the limit of a small quartic coupling. There are also attempts at higher loop order (See e.g. Ref. [25–27]) and based on the generalized Weinberg operator [28]. Now we would like to take a second look at the one-loop completions of the Weinberg operator and perform a systematic study and explore the possibility of $R\nu$ MDM.

This work is organized as follows: In Sec. 2 we discuss the one-loop topologies and determine the possible $R\nu$ MDM model realizations. In Sec. 3 we discuss one $R\nu$ MDM model and obtain an expression for neutrino mass. The relevant constraints from Higgs and flavor physics are elaborated on in Sec. 4 and electroweak-scale naturalness in Sec. 5. In Sec. 6 we discuss the allowed parameter space as well as other phenomenological issues, like collider phenomenology. We conclude in Sec. 7. Technical details are collected in the appendices.

2 One-Loop $R\nu$ MDM Models

Majorana neutrino masses can be conveniently expressed in the form of the Weinberg operator

$$\mathcal{O}_{\text{Weinberg}} = \frac{LLHH}{\Lambda}, \quad (1)$$

where Λ is the suppression scale and L and H denote the lepton and the Higgs doublets in the SM. The minimal UV completions of the Weinberg operator at tree level are the seesaw mechanisms. However the Weinberg operator can also be UV completed at loop level and neutrino mass is generated radiatively. A systematic study of the one-loop UV completions has been performed in Ref. [29]. Part of the one-loop completions also induce one of the seesaw mechanisms whose contribution is mostly dominant. These models are thus reducible and not genuine one-loop models. We show all the topologies that allow irreducible one-loop completions in Fig. 1. The well-known radiative seesaw model [6] is a realization of T3 shown in Fig. 1d. We want to first check the possibility to accommodate MDM in these topologies. A good $R\nu$ MDM model should at least satisfy the following three conditions:

1. At least one of the exotic particles in the loop should be a plausible MDM candidate, which can be either a fermionic quintuplet or a scalar septuplet with zero hypercharge [2].
2. Any exotic scalar with hypercharge $\pm\frac{1}{2}$ has to be in an odd-dimensional $SU(2)$ representation. Otherwise the quartic term $\phi^\dagger\phi(\phi^\dagger H + H^\dagger\phi)$ will spoil the accidental Z_2 symmetry.
3. The Lagrangian should of course be invariant under $SU(2)_L \times U(1)_Y$ before electroweak symmetry breaking. So the existence of the Yukawa interaction $L\chi_i\phi_i$ for fermions χ_i and scalars ϕ_i implies

$$d_{\phi_i} + d_{\chi_i} = 2n + 1, \quad (2)$$

where d_{ϕ_i} and d_{χ_i} denote the dimension of ϕ_i and χ_i , and n is a positive integer. Similarly a scalar trilinear coupling $\phi_i\phi_j H$ will result in

$$d_{\phi_i} + d_{\phi_j} = 2n + 1. \quad (3)$$

We discuss the four possible topologies in turn: For topology T1-i, any of the scalar field ϕ_i being a dark matter candidate will assign another scalar field ϕ_j with hypercharge $\pm\frac{1}{2}$ through

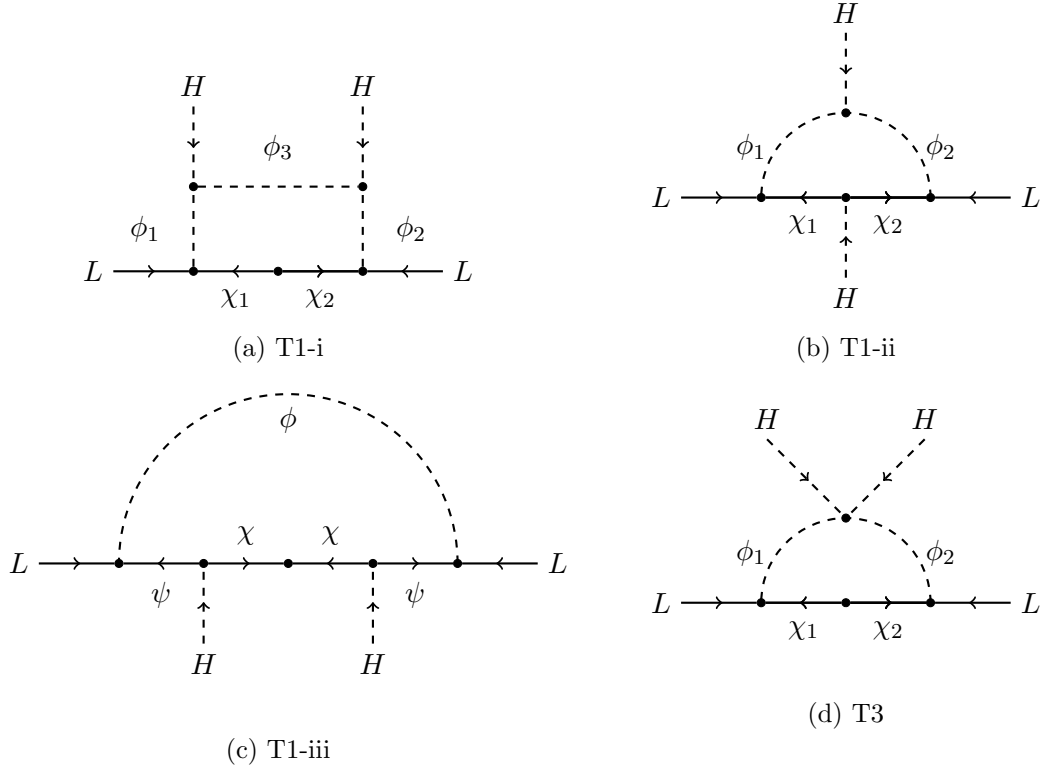


Figure 1: Irreducible one-loop topologies for minimal UV completions of the Weinberg operator.

trilinear scalar couplings $\phi_i\phi_jH$. So according to condition 1 and 2, both ϕ_i and ϕ_j are odd-dimensional, which violates condition 3. Alternatively χ_i can play the role of dark matter. This will also assign ϕ_i with hypercharge $\pm\frac{1}{2}$ through Yukawa interaction $L\chi_i\phi_i$. Similarly both χ_i and ϕ_i are odd-dimensional according to condition 1 and 2, which contradicts with condition 3. So topology T1-i does not provide any valid UV completion.

We follow the same argument for topology T1-ii. It suffices to consider either ϕ_1 or χ_2 to be a dark matter candidate as the diagram is symmetric. So the only possible assignment of hypercharges is $Y(\phi_1) = 0$, $Y(\phi_2) = -\frac{1}{2}$, $Y(\chi_1) = \frac{1}{2}$ and $Y(\chi_2) = 0$. We immediately notice that ϕ_2 has to be in an odd-dimensional representation according to condition 2. Therefore if ϕ_1 is the dark matter candidate, it must be an odd-dimensional representation of $SU(2)_L$ and does not satisfy condition 3. Alternatively if χ_2 is the dark matter candidate, it should be in an odd-dimensional representation and does not satisfy condition 3. So topology T1-ii is also ruled out.

For topology T1-iii, we find two minimal completions as shown in Tab. 1, one for scalar dark matter and one for fermion dark matter. Besides the exotic particles shown in the loop, another fermion $\bar{\psi}$ has to be introduced to cancel the anomaly and to write down a mass term.

We turn to topology T3 in the end. If we take χ_i to be dark matter candidate, ϕ_i should have hypercharge $\frac{1}{2}$ and thus be an odd-dimensional representation according to condition 2, which is contradicting with condition 3. This failed attempt is exactly the model considered in Ref. [23]. Another possibility is ϕ_i being the dark matter candidate. Again we can just take ϕ_1 due to the symmetry of the diagram. The quantum numbers of the exotic particles of the minimal UV completion of T3 are listed in Tab. 2. Non-minimal completions of T3 contain larger $SU(2)$ representations.

The last sanity check is to see if any renormalizable term invariant under the SM gauge group breaks the accidental Z_2 . For the completions shown in Tab. 1, the Yukawa coupling $\psi\bar{\psi}\phi$ spoils

Z_2 [30] as well as the cubic coupling ϕ^3 [2; 31]. Similarly $\chi_1\chi_2\phi_1$ and $\phi_1\phi_2^\dagger\phi_2$ for the model in Tab. 2 do the same [30]. Similar arguments apply to higher representations. Hence, there is no one-loop UV completion of the Weinberg operator in the framework of minimal dark matter, which leads to an exact accidental Z_2 symmetry. However, in the limit of vanishing renormalizable Z_2 -breaking couplings, the symmetry of the Lagrangian is enlarged and thus it is technically natural to have small Z_2 -breaking couplings [32]. All quantum corrections to these couplings are proportional to Z_2 -breaking couplings. With regards to minimal dark matter, the fermionic dark matter candidate is preferred [2]. We will consider the fermionic dark matter model in Tab. 1 and perform a detailed phenomenological study under the assumption that the Z_2 -breaking couplings are sufficiently small, such that the lifetime of χ is longer than the age of the Universe and satisfies all indirect detection constraints. Indirect detection constraints from photon, ν , e^+ and p^- searches are the strongest and generally require lifetimes $\tau_{DM} \gtrsim 10^{26}$ sec [33–36]. The maximum allowed size of the coupling can be estimated from the bound given in Eq. (13) in Ref. [30]

$$\tau_{DM} \lesssim 7.1 \times 10^8 \left(\frac{10^{-2}}{\lambda} \right)^2 \left(\frac{10^4 \text{GeV}}{m_{DM}} \right)^5 \left(\frac{m}{10^9 \text{GeV}} \right)^4 \text{sec}, \quad (4)$$

where λ denotes the Z_2 -breaking Yukawa coupling and m the mass of the particles in the loop. Taking $m \sim m_{DM}$, the bound on τ_{DM} can be translated to a bound on the Z_2 -breaking coupling, $\lambda \lesssim 3 \times 10^{-21}$. Despite the coupling being required to be extremely small, it is technically natural and quantum corrections will not induce larger Z_2 -breaking couplings. Thus the neutral component of χ constitutes a viable dark matter candidate. Note that besides the three models in Tabs. 1 and 2 there are other one-loop radiative neutrino mass models with a viable dark matter candidate including the original R ν MDM model [23].

3 The Model

The R ν MDM model with an approximate Z_2 symmetry, which we consider in this work, contains a real scalar quintuplet ϕ , two fermionic quadruplets ψ and $\bar{\psi}$, which form a Dirac pair, and a fermionic quintuplet χ . All even-dimensional SU(2) representations are pseudo-real and all odd ones are real. The higher-dimensional representations can be easily constructed using raising and lowering operators and we list the ones relevant for this model in Appendix B.

The real scalar quintuplet ϕ can be decomposed into electrical charge eigenstates as $\phi = (\phi^{++}, \phi^+, \phi^0, \phi^-, \phi^{--})^T$, where superscripts denote the electrical charges. The neutral component field ϕ^0 is a real scalar and the charged component fields $(\phi^+)^{\dagger} = \phi^-$, $(\phi^{++})^{\dagger} = \phi^{--}$ form two complex scalars. Similarly for the fermions, the component fields are defined as $\chi = (\chi^{++}, \chi^+, \chi^0, \chi^-, \chi^{--})^T$, $\psi = (\psi^{++}, \psi^+, \psi^0, \psi^-)^T$ and $\bar{\psi} = (\bar{\psi}^+, \bar{\psi}^0, \bar{\psi}^-, \bar{\psi}^{--})^T$.

Besides the SM part, the Lagrangian of this model consists of kinetic terms of the exotic particles and additional Yukawa interactions

$$\mathcal{L} = \mathcal{L}^{SM} + \mathcal{L}^{kin} + \mathcal{L}^{yuk}. \quad (5)$$

Spin of DM	χ	ψ	$\bar{\psi}$	ϕ
0	(5, 0)	(6, $\frac{1}{2}$)	(6, $-\frac{1}{2}$)	(7, 0)
$\frac{1}{2}$	(5, 0)	(4, $\frac{1}{2}$)	(4, $-\frac{1}{2}$)	(5, 0)

Table 1: Matter content of both the scalar and fermionic dark matter model for T1-iii and their quantum numbers under $SU(2)_L \times U(1)_Y$. Weyl notation is used.

Spin of DM	ϕ_1	ϕ_2	χ_1	χ_2
0	(7, 0)	(5, 1)	(6, $\frac{1}{2}$)	(6, $-\frac{1}{2}$)

Table 2: Matter content of the scalar dark matter model for T3 and their quantum numbers under $SU(2)_L \times U(1)_Y$. Weyl notation is used.

We leave the details of the kinetic terms to Appendix B as well. From the discussion later in this section, we know that more than one copy of ϕ is needed to explain both, the solar and the atmospheric, mass splittings. Thus we attach a subscript as the family indices ϕ_i . Then the Yukawa interactions are explicitly expressed in component fields as

$$\mathcal{L}^{yuk} = Y^H H^\dagger \psi \chi + \sum_{i,j} Y_{ij}^L L_i \psi \phi_j + h.c. \quad (6)$$

$$= \frac{Y^H}{2} \left\{ H^- \left(2\chi^{++}\psi^- - \sqrt{3}\chi^+\psi^0 + \sqrt{2}\chi^0\psi^+ - \chi^-\psi^{++} \right) \right. \\ \left. + (H^0)^\dagger \left(\chi^+\psi^- - \sqrt{2}\chi^0\psi^0 + \sqrt{3}\chi^-\psi^+ - 2\chi^{--}\psi^{++} \right) \right\} \quad (7)$$

$$+ \frac{Y_{ij}^L}{2} \left\{ e_i \left(2\phi_j^{++}\psi^- - \sqrt{3}\phi_j^+\psi^0 + \sqrt{2}\phi_j^0\psi^+ - \phi_j^-\psi^{++} \right) \right. \\ \left. + \nu^i \left(-\phi_j^+\psi^- + \sqrt{2}\phi_j^0\psi^0 - \sqrt{3}\phi_j^-\psi^+ + 2\phi_j^{--}\psi^{++} \right) \right\} + h.c. . \quad (8)$$

Without loss of generality we can choose Y^H to be real and positive using a phase redefinition of ψ . Similarly three phases of Y_{ij}^L can be absorbed by a phase redefinition of L_i .

Apparently the Yukawa interaction in Eqn. (7) will induce mixing in the fermion sector. The mass matrix for the neutral sector in basis $\Psi^0 = (\psi^0, \bar{\psi}^0, \chi^0)$ is

$$M_0 = \begin{pmatrix} 0 & m_\psi & \frac{1}{2}Y^H v \\ m_\psi & 0 & 0 \\ \frac{1}{2}Y^H v & 0 & m_\chi \end{pmatrix}, \quad (9)$$

where $v = 246$ GeV is the vev of the Higgs boson. Similarly the mass matrix for the singly charged fermions in the basis $(\psi^+, \bar{\psi}^+, \chi^+, \psi^-, \bar{\psi}^-, \chi^-)$ reads

$$M_1 = \begin{pmatrix} 0 & X_1 \\ X_1^T & 0 \end{pmatrix} \quad X_1 = \begin{pmatrix} 0 & -m_\psi & -\frac{\sqrt{3}}{2\sqrt{2}}Y^H v \\ -m_\psi & 0 & 0 \\ -\frac{1}{2\sqrt{2}}Y^H v & 0 & -m_\chi \end{pmatrix}. \quad (10)$$

The doubly-charged fermions also mix through the Yukawa interaction. In the basis of interaction eigenstates $(\psi^{++}, \chi^{++}, \bar{\psi}^{--}, \chi^{--})$, the mass matrix reads

$$M_2 = \begin{pmatrix} 0 & X_2 \\ X_2^T & 0 \end{pmatrix} \quad X_2 = \begin{pmatrix} m_\psi & \frac{1}{\sqrt{2}}Y^H v \\ 0 & m_\chi \end{pmatrix}. \quad (11)$$

The diagonalization of these mass matrices can be done using the Takagi factorization and singular value decomposition, respectively. The details of which are collected in Appendix A.

The neutral component of χ is the dark matter candidate of this model. To saturate the dark matter density observed by Planck [37], the dark matter mass should be [38]

$$m_\chi = (9.4 \pm 0.47) \text{ TeV}, \quad (12)$$

where Sommerfeld effects have been taken into account [2]. Other dark sector particles have to be heavier than m_χ , which makes the mixing between χ and ψ , roughly given by $Y^H v/m_{\chi,\psi}$, negligible.

The neutrino mass after electroweak symmetry breaking is defined by $\mathcal{L} = -\frac{1}{2}m_\nu\nu\nu$ and thus

$$(m_\nu)_{ij} = \frac{(Y^H v)^2 m_\chi}{256\pi^2 m_\psi^2} \sum_k Y_{ik}^L Y_{jk}^L g\left(\frac{m_{\phi_k}^2}{m_\psi^2}, \frac{m_\chi^2}{m_\psi^2}\right) \quad (13)$$

with the factor

$$g(\eta_1, \eta_2) = \frac{1}{(1-\eta_1)(1-\eta_2)} + \frac{1}{\eta_1 - \eta_2} \left(\frac{\eta_1^2 \ln \eta_1}{(1-\eta_1)^2} - \frac{\eta_2^2 \ln \eta_2}{(1-\eta_2)^2} \right). \quad (14)$$

The calculation is done neglecting mass mixing among the fermions which could only give rise to a tiny correction proportional to $Y^H v/m_{\chi,\psi}$. The neutrino mass matrix m_ν is full rank if and only if $n_\phi \geq 3$. The Yukawa couplings Y^L can be expressed as

$$Y_{ij}^L = \frac{16\pi m_\psi}{Y^H v \sqrt{m_\chi}} \sum_{k,l} (V_\nu^*)_{ik} \left(\hat{m}_\nu^{\frac{1}{2}} \right)_{kl} \mathcal{O}_{lj} g_j^{-\frac{1}{2}} \quad (15)$$

using a Casas-Ibarra-type parametrisation [39], where \mathcal{O} is a general complex orthogonal matrix and U diagonalises the neutrino mass matrix with $\hat{m}_\nu = V_\nu^T m_\nu V_\nu$.

To keep minimality, we will only introduce two copies of ϕ , which suffices to explain the solar and atmospheric mass splittings. One of the neutrinos remains massless. Both Y^L and \mathcal{O} are 3×2 matrices. The Yukawa couplings Y^L are entirely determined by the solar and atmospheric mass squared differences and the leptonic mixing parameters. The only relevant undetermined parameter is a complex angle θ parameterising the 3×2 orthogonal matrix \mathcal{O} . The two elements of the orthogonal matrix \mathcal{O} associated with the massless neutrino do not enter the Yukawa coupling Y^L . Neutrino mass fixes the product of the Yukawa couplings $Y_{ij}^L Y^H$. We will study the phenomenology induced by these Yukawa couplings and work out the experimental constraints on the model parameter space in the following sections.

4 Constraints from Higgs physics and flavor physics

The Yukawa interactions introduced in Eqn. (6) modify the SM in two aspects: The coupling between the SM Higgs and the exotic particles will change the decay width of the Higgs; Lepton family number is also violated and lead to lepton flavor-changing rare processes. Both impose constraints on the parameter space of the model. Since exotic particles introduced are not charged under $SU(3)_c$, there will be no new contribution to processes such as meson mixings and $b \rightarrow s$ transition. Derivation of the constraints involves calculation of one-loop Feynman diagrams, which is assisted by the Mathematica packages FeynRules [40], FeynArts [41], FormCalc [42], and ANT [43]

4.1 Constraints from the Higgs

The Yukawa coupling Y^H can modify the behavior of the Higgs boson. As all exotic particles are colorless, the production of the Higgs at the LHC is untouched. The decay from the Higgs to the exotic particles is also forbidden kinematically. However, the exotic particles can contribute to the decay of the Higgs at loop level such as $h \rightarrow \gamma\gamma$ or $h \rightarrow Z\gamma$ as depicted in Fig. 2. LHC has measured the production of the Higgs boson in the diphoton channels. Among them the diphoton

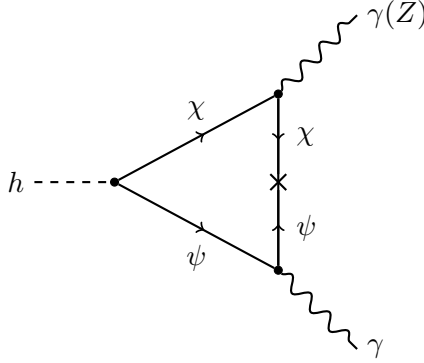


Figure 2: Higgs decays to two bosons at one loop with exotic fermions. There are similar diagrams with the mass insertion on the other two edges of the fermion triangle.

measurement is the most accurate one, which we will use to derive our constraint. The Higgs signal strength in the diphoton channel is defined as

$$\mu = \frac{\Gamma_{h \rightarrow \gamma\gamma}^{\text{R}\nu\text{MDM}}}{\Gamma_{h \rightarrow \gamma\gamma}^{\text{SM}}}, \quad (16)$$

with the decay width of Higgs to diphoton in this model

$$\Gamma_{h \rightarrow \gamma\gamma}^{\text{R}\nu\text{MDM}} = \frac{G_F \alpha^2 m_h^3}{128 \sqrt{2} \pi^3} \left| F_1\left(\frac{4m_W^2}{m_h^2}\right) + \sum_f N_c Q_f^2 F_{\frac{1}{2}}\left(\frac{4m_f^2}{m_h^2}\right) + \frac{10 \times |Y^H|^2 m_t v}{m_\chi^2} I\left(\frac{m_\psi^2}{m_\chi^2}\right) \right|^2, \quad (17)$$

where the first two terms are the well-known results for the contributions from W boson and the SM fermions, and the last term is the new contribution from the Yukawa interaction $H^\dagger \psi \chi$. $\Gamma_{h \rightarrow \gamma\gamma}^{\text{SM}}$ can be achieved by simply setting Y^H to be zero in Eqn. (17). The dimensionless loop factors in Eqn. (17) are

$$F_1(\tau) = 2\tau + 3\tau + 3\tau(2 - \tau)f(\tau), \quad F_{\frac{1}{2}}(\tau) = -2\tau(1 + (1 - \tau)f(\tau)),$$

$$I(\eta) = \frac{(\eta + 1)(\eta^3 + 9\eta^2 - 9\eta - 1 - 6\eta(\eta + 1)\ln \eta)}{6(\eta - 1)^5}, \quad (18)$$

where $f(\tau) = \sin^{-1}(\sqrt{1/\tau})$ and $I(\eta)$ has been obtained in the limit $m_\chi, m_\psi \gg m_h$. We derive the limit on Y^H for specific fermion masses from $\mu = 1.17_{-0.17}^{+0.19}$ [44]. In Fig. 3 we plot the contours of the maximal Y^H allowed by the measurements at the LHC in solid lines. As the exotic particles have masses of 9.4 TeV to saturate the relic density, the current experiments impose literally no constraints on Y^H . We also project the future constraints on Y^H at 14 TeV LHC with 3000 fb^{-1} dataset. An optimistic estimate of 5% sensitivity [45] is used to extract the limits shown in the dashed contours also in Fig. 3. However, the heavy masses of the exotic particles make it impossible to place any meaningful constraints on Y^H even at the high luminosity (HL) -LHC.

4.2 Lepton Flavor Violating Processes

The Yukawa interaction in Eqn. (8) will induce lepton flavor violating (LFV) processes. Several LFV processes, such as $\mu^- \rightarrow e^- \gamma$, $\mu \rightarrow eee$ and μ - e conversion in nuclei, have been probed with extremely high sensitivity, but no signal has been found. The experimental results will surely place strong constraints on the model parameters. We will study the most well measured and thus most stringent ones in this section. The implications of these constraints will be discussed in Sec. 6.

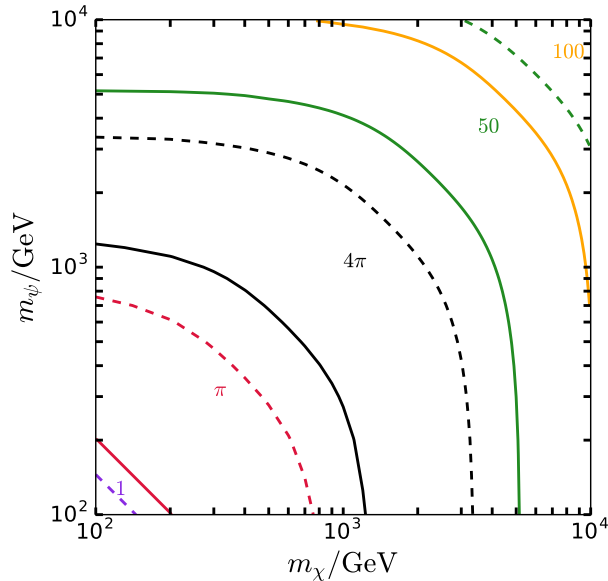


Figure 3: Contour plot of the maximal Y^H allowed by the measurement of the signal strength of $h \rightarrow \gamma\gamma$. The solid contours denotes the current limit and the dashed from the future 3000 fb^{-1} LHC, where purple, red, black, green and yellow lines correspond to 1, π , 4π , 50 and 100.

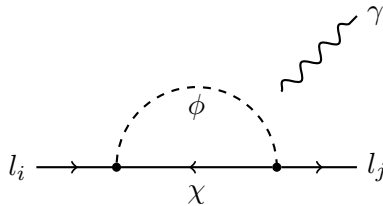


Figure 4: Feynman diagram for $l_i \rightarrow l_j \gamma$ where the emitted photon can be attached to any charged particles in the diagram.

4.2.1 $l_i \rightarrow l_j \gamma$

We consider the process of the form $l_i \rightarrow l_j \gamma$ first and follow the convention in Ref. [46]. This type of decay is rare compared with the dominant tree-level decay via a virtual W boson. The amplitude of such process, depicted in Fig. 4, reads

$$\mathcal{M}(l_i \rightarrow l_j \gamma) = e \epsilon_\mu^* \bar{u}(p_j) i \sigma^{\mu\nu} q_\nu (\sigma_{Lij} P_L + \sigma_{Rij} P_R) u(p_i), \quad (19)$$

where e is the magnitude of electron charge and $P_{L,R} \equiv \frac{1}{2} (1 \mp \gamma_5)$ are the projection operators. The coefficients $\sigma_{Lij,Rij}$ can be written as

$$\sigma_{Lij} = \frac{m_{l_j}}{16\pi^2} \sum_k \frac{Y_{ik}^L Y_{jk}^{L*}}{m_{\phi_k}^2} F\left(\frac{m_\psi^2}{m_{\phi_k}^2}\right), \quad \sigma_{Rij} = \frac{m_{l_i}}{16\pi^2} \sum_k \frac{Y_{ik}^L Y_{jk}^{L*}}{m_{\phi_k}^2} F\left(\frac{m_\psi^2}{m_{\phi_k}^2}\right), \quad (20)$$

where $F(\eta)$ is defined as

$$F(\eta) = \frac{5(1 - 6\eta + 3\eta^2 + 2\eta^3 - 6\eta^2 \ln \eta)}{24(\eta - 1)^4}. \quad (21)$$

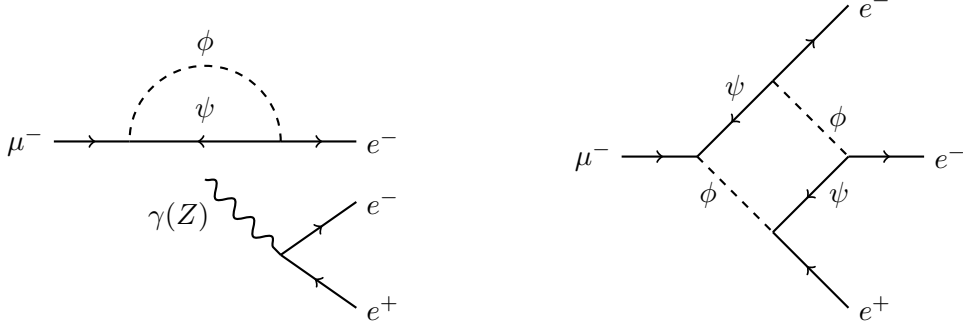


Figure 5: Feynman diagrams for $\mu^- \rightarrow e^- e^+ e^-$: γ - or Z -penguins on the left and the box diagram on the right.

The partial width then can be easily calculated with

$$\Gamma(l_i \rightarrow l_j \gamma) = \frac{(m_{l_i}^2 - m_{l_j}^2)^3 e^2 (|\sigma_L|^2 + |\sigma_R|^2)}{16\pi m_{l_i}^3} \quad (22)$$

In the minimal variant of the model with two scalar quintuplets only, the relative rates are fixed and they are of similar order of magnitude. The current experimental limits are given by $\text{Br}(\mu \rightarrow e\gamma) < 5.7 \times 10^{-13}$ [47], $\text{Br}(\tau \rightarrow e\gamma) < 3.3 \times 10^{-8}$ and $\text{Br}(\tau \rightarrow \mu\gamma) < 4.4 \times 10^{-8}$ [44]. Thus the most constraining limit is from $\mu \rightarrow e\gamma$, which we will discuss in Sec. 6. The proposed upgrade of MEG will improve the future sensitivity of $\mu \rightarrow e\gamma$ down to $\text{Br}(\mu \rightarrow e\gamma) \sim 6 \times 10^{-14}$ [48].

4.2.2 Anomalous Magnetic Moment

The lepton anomalous magnetic moment can also be expressed with the terms in Eqn. (20)

$$\Delta a_i = 2 e m_{l_i} (\sigma_{Lii} + \sigma_{Rii}) = \frac{e}{4\pi^2} \sum_k |Y_{ik}^L|^2 \frac{m_{l_i}^2}{m_{\phi_k}^2} F\left(\frac{m_{\psi}^2}{m_{\phi_k}^2}\right). \quad (23)$$

The anomalous magnetic moment of the muon has been measured to a very high precision $\Delta a_\mu = 0.0011659209 \pm 0.0000000006$ [49]. Given the heavy scalar quintuplet masses, the correction to the anomalous magnetic moment of the muon is well below the experimental precision and thus it does not impose any constraint.

4.2.3 $\mu \rightarrow eee$

Another well-measured LFV process is $\mu \rightarrow eee$, which this model will have several different contributions including γ -penguin, Z -penguin, Higgs-penguin, and box diagrams. The contribution from the Higgs-penguin is proportional to the electron mass and negligible. We show the relevant Feynman diagrams for this process in Fig. 5. The amplitude of the γ -penguin can be written in the form of

$$\begin{aligned} \mathcal{M}_\gamma &= \bar{u}(p_1) (q^2 \gamma_\mu (A_1^L P_L + A_1^R P_R) + i m_\mu \sigma_{\mu\nu} q^\nu (A_2^L P_L + A_2^R P_R)) u(p) \\ &\times \frac{e^2}{q^2} \bar{u}(p_2) \gamma^\mu v(p_3) - (p_1 \leftrightarrow p_2) , \end{aligned} \quad (24)$$

where p is the momentum of the initial muon and $p_{1,2,3}$ are the momenta of the two electrons and the positron in the final state. The loop functions are given by

$$A_1^L = \frac{1}{16\pi^2} \sum_k \frac{Y_{2k}^L Y_{1k}^{L*}}{m_{\phi_k}^2} G\left(\frac{m_\psi^2}{m_{\phi_k}^2}\right), \quad G(\eta) = \frac{5(2 - 9\eta + 18\eta^2 - 11\eta^3 + 6\eta^3 \ln \eta)}{72(\eta - 1)^4}, \quad (25)$$

$$A_1^R = 0, \quad A_2^{L,R} = \frac{\sigma_{L21,R21}}{m_\mu}, \quad (26)$$

where we have set the electron mass and the external momenta to zero. Similarly the contribution from the Z -penguin is

$$\mathcal{M}_Z = \frac{1}{m_Z^2} \bar{u}(p_1) \gamma_\mu (F_L P_L + F_R P_R) u(p) \times \bar{u}(p_2) \gamma^\mu (Z_L^e P_L + Z_R^e P_R) v(p_3) - (p_1 \leftrightarrow p_2), \quad (27)$$

$$F_L = \sum_k \frac{1}{16\pi^2} \frac{e Y_{2k}^L Y_{1k}^{L*}}{\sin \theta_W \cos \theta_W} H\left(\frac{m_\psi^2}{m_{\phi_k}^2}\right), \quad F_R = 0, \quad H(\eta) = \frac{5\eta(1 - \eta + \ln \eta)}{4(\eta - 1)^2}, \quad (28)$$

where $Z_{L,R}^e$ is the weak charge of the left- or right-handed electron. The weak charge of any fermion f is defined as

$$Z_{L,R}^f = \frac{e}{\sin \theta_W \cos \theta_W} \left(T_3^{fL,fR} - Q_f \sin^2 \theta_W \right) \quad (29)$$

with $T_3^{fL,fR}$ being the isospin of $f_{L,R}$ and Q_f the electrical charge of f . Finally the leading order contribution from the box diagram can be written as

$$\mathcal{M}_{Box} = e^2 B_1^L [\bar{u}(p_1) \gamma^\mu P_L u(p)] [\bar{u}(p_2) \gamma_\mu P_L v(p_3)] - (p_1 \leftrightarrow p_2), \quad (30)$$

where we have neglected subdominant contributions further suppressed by the heavy mass scale and the loop function B_1^L is

$$B_1^L = \sum_{i,j} \frac{1}{16\pi^2} \frac{5Y_{2m}^L Y_{1n}^{L*} Y_{1m}^{L*} Y_{1n}^L}{4} D_{00} \left[m_\psi^2, m_\psi^2, m_{\phi_i}^2, m_{\phi_j}^2 \right]. \quad (31)$$

The analytic expression of the four-point function D_{00} can be found in the Appendix of Ref. [43]. Among the various contributions, only the Z -penguin is suppressed by the Z boson mass, while the others are all suppressed by the masses of the exotic particles. With the amplitude we can easily write down the decay width [50–52],

$$\begin{aligned} \Gamma(\mu^- \rightarrow e^- e^+ e^-) &= \frac{e^4 m_\mu^5}{512\pi^3} \times \left[|A_1^L|^2 + (|A_2^L|^2 + |A_2^R|^2) \left(\frac{16}{3} \ln \frac{m_\mu}{m_e} - \frac{22}{3} \right) \right. \\ &\quad + \frac{1}{6} |B_1^L|^2 + \frac{2}{3} |F_{LL}|^2 + \frac{1}{3} |F_{LR}|^2 - 2(A_1^L A_2^{R*} + h.c.) \\ &\quad + \frac{1}{3} (A_1^L B_1^{L*} - 2A_2^R B_1^{L*} + h.c.) + \frac{1}{3} (2A_1^L F_{LL}^* + A_1^L F_{LR}^* h.c.) \\ &\quad \left. + \frac{1}{3} (B_1^L F_{LL}^*) - \frac{2}{3} (2A_2^R F_{LL}^* + A_2^R F_{LR}^* + h.c.) \right], \quad (32) \end{aligned}$$

with the factors $F_{LL,LR} = F_L Z_{L,R}^e / (e m_Z)^2$, where we have omitted all the vanishing or next-to-leading order contributions. The heavy exotic particles in this model imply that the Z -penguin contribution dominates over the contributions of the γ -penguin and the box diagrams. The branching ratio for this rare decay channel can be approximately obtained by dividing Eqn. (32) by the decay width of $\mu^- \rightarrow e^- \bar{\nu}_e \nu_\mu$. The current experimental limit is given by $\text{Br}(\mu \rightarrow eee) < 10^{-12}$ [53] and there is a proposal for an experiment with an substantially increased sensitivity down to $\text{Br}(\mu \rightarrow eee) < 10^{-16}$ [54].

4.2.4 μ - e Conversion in Nuclei

The last LFV process we consider is μ - e conversion in nuclei. There are two types of contributions: the long-range interactions determined by the electromagnetic dipole, and the short-range interactions from the penguin diagrams as shown in Fig. 5 with the final electron pair replaced by a quark pair. For this model, there is no contribution from the box diagrams because no colored exotic states are introduced. Therefore the effective Lagrangian can be expressed as

$$\begin{aligned} \mathcal{L}_{eff} = & -\frac{1}{2}m_\mu (A_2^L \bar{e}\sigma^{\mu\nu} P_L \mu F_{\mu\nu} + A_2^R \bar{e}\sigma^{\mu\nu} P_R \mu F_{\mu\nu} + h.c.) \\ & - \sum_{q=u,d,s} [(g_{LV(q)} \bar{e}\gamma^\mu P_L \mu) \bar{q}\gamma_\mu q + (g_{LA(q)} \bar{e}\gamma^\mu P_L \mu) \bar{q}\gamma_\mu \gamma_5 q + h.c.] , \end{aligned} \quad (33)$$

where the first and second lines denote the long- and short-range interactions. The Wilson coefficients $g_{LV(q)}$ only receive a contribution from the γ -penguin, while $g_{LA(q)}$ from both γ - and Z -penguins. They can be written as

$$g_{LV(q)}^\gamma = \frac{e^2 Q_q}{16\pi^2} \sum_i \frac{Y_{2i}^L Y_{1i}^{L*}}{m_{\phi_i}^2} G\left(\frac{m_\psi^2}{m_{\phi_i}^2}\right), \quad (34)$$

$$g_{LV(q),LA(q)}^Z = -\frac{e}{16\pi^2} \frac{\pm Z_L^q + Z_R^q}{\sin\theta_W \cos\theta_W} \sum_i \frac{Y_{2i}^L Y_{1i}^{L*}}{m_Z^2} H\left(\frac{m_\psi^2}{m_{\phi_i}^2}\right), \quad (35)$$

where Q_f is the electrical charge of the quarks. Similar to $\mu \rightarrow eee$ the Z -penguin contribution dominates over the γ -penguin. Coherent processes generally dominate over incoherent processes, if the final state nucleus is the same as the initial state nucleus. Thus we will focus on coherent contributions to μ - e conversion and neglect any incoherent contribution. So the conversion rate is [55]

$$\omega_{conv} = 4 \left| \frac{1}{8} A_2^{R*} D + \tilde{g}_{LV}^{(p)} V^{(p)} + \tilde{g}_{LV}^{(n)} V^{(n)} \right|^2 + 4 \left| \frac{1}{8} A_2^{L*} D \right|^2, \quad (36)$$

where $\tilde{g}_{LV}^{(p,n)}$ are the coefficients of the vector interactions with protons and neutrons defined as $\tilde{g}_{LV}^{(p)} = 2g_{LV(u)} + g_{LV(d)}$ and $\tilde{g}_{LV}^{(n)} = g_{LV(u)} + 2g_{LV(d)}$. We use the values in Tab. 1 of Ref. [55] for the overlap integrals D , $V^{(p)}$ and $V^{(n)}$. The branching ratio of μ - e conversion is defined as the ratio between the conversion rate and the capture rate

$$\text{Br}(\mu N \rightarrow e N) \equiv \frac{\omega_{conv}}{\omega_{capt}}, \quad (37)$$

where the rate ω_{capt} takes the value $13.07 \times 10^6 s^{-1}$, $2.59 \times 10^6 s^{-1}$ and $0.7054 \times 10^6 s^{-1}$ in Au, Ti and Al [55]. The current bounds on the branching ratio are $\text{Br}(\mu\text{Au} \rightarrow e\text{Au}) < 7 \times 10^{-13}$ and $\text{Br}(\mu\text{Ti} \rightarrow e\text{Ti}) < 4.3 \times 10^{-12}$ [44]. There are good prospects to increase the future sensitivities for Al and Ti to $\text{Br}(\mu\text{Al} \rightarrow e\text{Al}) \lesssim 10^{-16}$ [56–60] and $\text{Br}(\mu\text{Ti} \rightarrow e\text{Ti}) \lesssim 10^{-18}$ [56; 57], respectively.

5 Naturalness

The newly introduced particles lead to corrections to the Higgs effective potential. Defining the tree-level Higgs potential as

$$V(H) = -\mu_H^2 H^\dagger H + \lambda (H^\dagger H)^2 \quad (38)$$

with the Higgs vev $\langle H \rangle = v/\sqrt{2}$ and the Higgs mass m_h^2 , the minimization conditions give

$$v^2 = \frac{\mu_H^2}{\lambda}, \quad \text{and} \quad m_h^2 = 4\mu_H^2 = 4\lambda v^2. \quad (39)$$

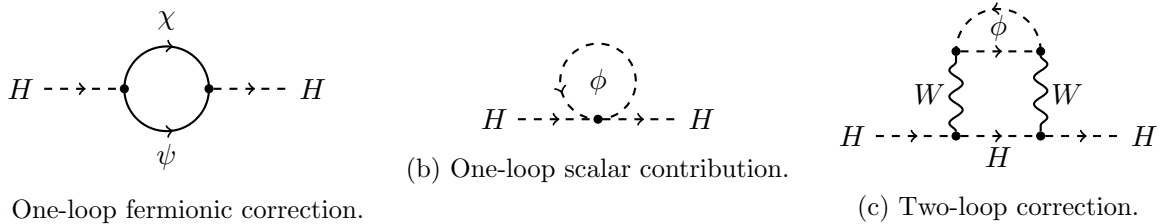


Figure 6: Corrections to Higgs bilinear from new particles in the theory.

In order to estimate the corrections of the new particles on electroweak scale naturalness, we calculate the corrections to the Higgs bilinear in the scalar potential. The correction to the quartic term is dimensionless and is not quadratically enhanced by the heavy mass scale compared to the electroweak scale. We use dimensional regularization with the modified minimal subtraction (\overline{MS}) renormalization scheme to calculate the one-loop correction given in Fig. 6a. After canceling the divergent part with the counterterm, there is a finite contribution to the effective bilinear term of the Higgs $\mu_{H,eff}^2 = \mu_H^2 + \delta\mu_H^2$ with

$$\delta\mu_H^2|_{\text{fermion}} = -\frac{(Y^H)^2}{8\pi^2} \left(m_\chi^2 \left(2 - \frac{2m_\chi^2 - m_\psi^2}{m_\chi^2 - m_\psi^2} \ln \frac{m_\chi^2}{\mu^2} \right) + m_\psi^2 \left(2 - \frac{2m_\psi^2 - m_\chi^2}{m_\psi^2 - m_\chi^2} \ln \frac{m_\psi^2}{\mu^2} \right) \right) \quad (40)$$

Thus it receives a quadratic correction from the new fermions in the loop. This poses a naturalness problem. The correction to the quartic coupling is of order $(Y^H)^4$, but does not receive a quadratic enhancement by the large mass hierarchy.

Similarly the Higgs couples to the scalar ϕ leading to a one-loop correction to the Higgs mass, which is shown in Fig. 6b. This quartic coupling, however, is unrelated to neutrino mass and could in principle be arbitrarily small at a given renormalization scale. Thus the two-loop contribution is effectively the leading order contribution related to ϕ , that we take into account.

In the unbroken phase its main contribution is given by diagrams of the type shown in Fig. 6c with W bosons and ϕ in the loop, which we estimate as follows

$$\delta\mu_H^2|_{\text{scalar}} \simeq g^4 C \left(\frac{1}{16\pi^2} \right)^2 A_0(m_\phi^2) = \frac{C \alpha_2^2}{16\pi^2} m_\phi^2 \left(\frac{1}{\epsilon} + 1 - \ln \frac{m_\phi^2}{\mu^2} \right). \quad (41)$$

The constant C is an order one factor, which we do not explicitly determine. We will naively set it to 1 in the following for simplicity, which is enough for an order of magnitude estimate.

Evaluating the expression for the Higgs mass at the scale $\mu = m_h$

$$m_h^2 = 4\mu_{H,eff}^2 = 4\mu_H^2 - \frac{(Y^H)^2}{2\pi^2} \left(m_\chi^2 \left(2 - \frac{2m_\chi^2 - m_\psi^2}{m_\chi^2 - m_\psi^2} \ln \frac{m_\chi^2}{m_h^2} \right) + m_\psi^2 \left(2 - \frac{2m_\psi^2 - m_\chi^2}{m_\psi^2 - m_\chi^2} \ln \frac{m_\psi^2}{m_h^2} \right) \right) + \frac{C \alpha_2^2}{4\pi^2} m_\phi^2 \left(1 - \ln \frac{m_\phi^2}{m_h^2} \right) \quad (42)$$

The required fine-tuning to arrange for the correct Higgs mass by canceling the finite correction with the term tree-level term μ_H^2 can be estimated by Δ^{-1} with

$$\Delta^2 \equiv \sum_{i=\chi,\psi,\phi} \left(\frac{\partial \ln m_h^2}{\partial \ln m_i^2} \right)^2 = \sum_{i=\chi,\psi,\phi} \left(\frac{m_i^2}{m_h^2} \frac{\partial m_h^2}{\partial m_i^2} \right)^2, \quad (43)$$

which quantifies the amount of tuning required to obtain the correct Higgs mass.

6 Discussion

Currently the LUX dark matter experiment [61] places the strongest limit on the dark matter direct detection cross section. Despite the mixing with ψ , there is no tree-level contribution to the spin-independent cross section from Z -boson exchange due to the Majorana nature of the dark matter candidate. Thus the dominant contribution arises from loop-level processes [2; 62]. The limit on dark matter direct detection cross section is given up to 1 TeV, which is roughly 10^{-44} cm². If we extrapolate the limit to the quintuplet mass, 9.4 TeV, the limit will be much weaker and thus will not put any constraint on this model at the moment. This model, however, will be probed by future direct detection experiments such as XENON 1T [63].

Dark matter annihilation in our galaxy produces high energy gamma rays. Experiments such as High Energy Stereoscopic System (H.E.S.S) [64] and the planned Cherenkov Telescope Array (CTA) [65] are searching for such signals and can place limits on the model. This limit on quintuplet has been discussed in Refs. [38; 66; 67] thoroughly. It is in tension with the current observation for a cuspy profile of dark matter halo, but allowed for a cored one. Nevertheless, this model is within the reach of the future CTA independent of the dark matter profile and will be tested soon.

The possibility to test MDM at a collider has been extensively studied for the LHC, the HL-LHC and even a 100 TeV proton-proton collider [68; 69]. Generally electroweak multiplets can be tested in events with mono-jet, mono-photon, vector-boson fusion and disappearing tracks. Among them, the test with disappearing tracks has the best sensitivity, with a reach of about 3 TeV for a 100 TeV proton-proton collider for an integrated luminosity of 30 ab⁻¹, which is still far below the mass of the dark matter candidate of this model.

Lepton flavor violating processes are governed by the Yukawa coupling Y^L , while the Higgs to diphoton branching ratio and naturalness are controlled by Y^H . Finally, neutrino mass depends on the product of Yukawa couplings $Y^H Y^L$ and thus connects the phenomenology creating an interesting interplay. The smaller Y^H , the larger Y^L and consequently the larger the LFV branching ratios. In Fig. 7 we show the branching ratio for the lepton flavor violating processes $\mu \rightarrow e\gamma$ (red), $\mu \rightarrow eee$ (green), and μ - e conversion² in gold (blue), aluminium (maroon), and titanium (magenta) as a function of Y^H for fixed masses $m_\chi = 9.4$ TeV, $m_\psi = 15$ TeV, $m_{\phi_1} = 16$ TeV, and $m_{\phi_2} = 16.5$ TeV as solid lines. The dotted lines indicate the change if the masses of ψ and ϕ_i are doubled. The solar and atmospheric mass squared differences and the leptonic mixing parameters are fixed to the best-fit values of v2.0 of the nu-fit collaboration [70]. Leptonic CP phases are set to zero, as well as the complex angle θ parameterizing \mathcal{O} . The horizontal solid lines show the current experimental bounds on $\text{Br}(\mu \rightarrow e\gamma) < 5.7 \times 10^{-13}$ [47] (red), $\text{Br}(\mu \rightarrow eee) < 10^{-12}$ [53] (green), $\text{Br}(\mu\text{Ti} \rightarrow e\text{Ti}) < 4 \times 10^{-13}$ [71] (magenta), and $\text{Br}(\mu\text{Au} \rightarrow e\text{Au}) < 7 \times 10^{-13}$ [72] (blue), while the dashed lines indicate the future sensitivities: $\text{Br}(\mu \rightarrow e\gamma) \sim 6 \times 10^{-14}$ [48], $\text{Br}(\mu \rightarrow eee) \sim 10^{-16}$ [54], $\text{Br}(\mu\text{Al} \rightarrow e\text{Al}) \sim 10^{-16}$ [56–60]) and $\text{Br}(\mu\text{Ti} \rightarrow e\text{Ti}) \sim 10^{-18}$ [56; 57]. For fixed masses and Yukawa coupling Y^H , it is possible to quantify how much the parameters of the model have to be tuned to obtain the electroweak scale. We show the required fine-tuning Δ^{-1} , which is defined in Eqn. (43), as a black solid line for our benchmark point and dotted line for doubled particle masses. The values can be read off the y-axis on the right-hand side. The Yukawa coupling Y^H becomes non-perturbative on the right-hand side of the figure, while the largest entry of the Yukawa coupling Y^L becomes non-perturbative on the left-hand side of the figure. We plot the maximum value of the Yukawa couplings, $\max(Y_{ij}^L, Y^H)$, in gray. The value can be read off the y-axis on the right-hand side.

Fig. 8 illustrates the uncertainty in the solar and atmospheric mass squared differences and leptonic mixing parameters. All these parameters are varied within their 3σ allowed ranges. The

²We use the values of Tab. 1 of Ref. [55] for the overlap integrals. A comparison of the rates for the overlap integral values in Tabs. 2 and 4 of [55] indicates an uncertainty of about 44%, 5%, and 11% for Au, Al, and Ti, respectively.

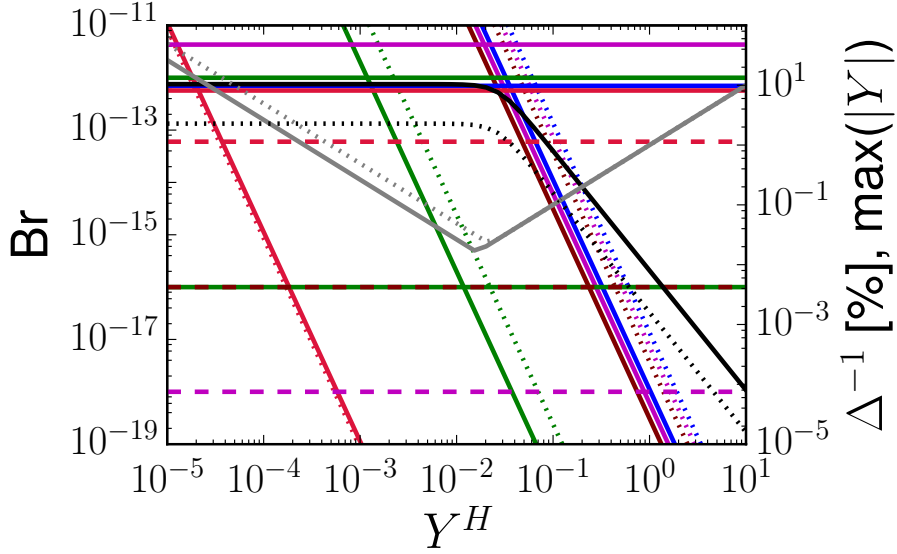


Figure 7: Prediction for lepton flavor violating processes $\mu \rightarrow e\gamma$ (red) , $\mu \rightarrow eee$ (green), and μ - e conversion in gold (blue), aluminium (maroon) and titanium (magenta). The horizontal solid lines indicate the current experimental bound, while the dashed line indicates the future sensitivity of proposed experiments. The required fine-tuning Δ^{-1} is shown in black and the maximum value of the Yukawa couplings, $\max(Y_{ij}^L, Y^H)$, in gray. The solid lines are for $m_\chi = 9.4$ TeV, $m_\psi = 15$ TeV, $m_{\phi_1} = 16$ TeV, and $m_{\phi_2} = 16.5$ TeV, while the dotted lines indicate the change if the masses of ψ and ϕ_i are doubled. The leptonic mixing parameters and neutrino mass squared differences are fixed to their best-fit values. We use v2.0 of the nu-fit collaboration [70]. Leptonic CP phases and the complex angle θ in \mathcal{O} are set to zero.

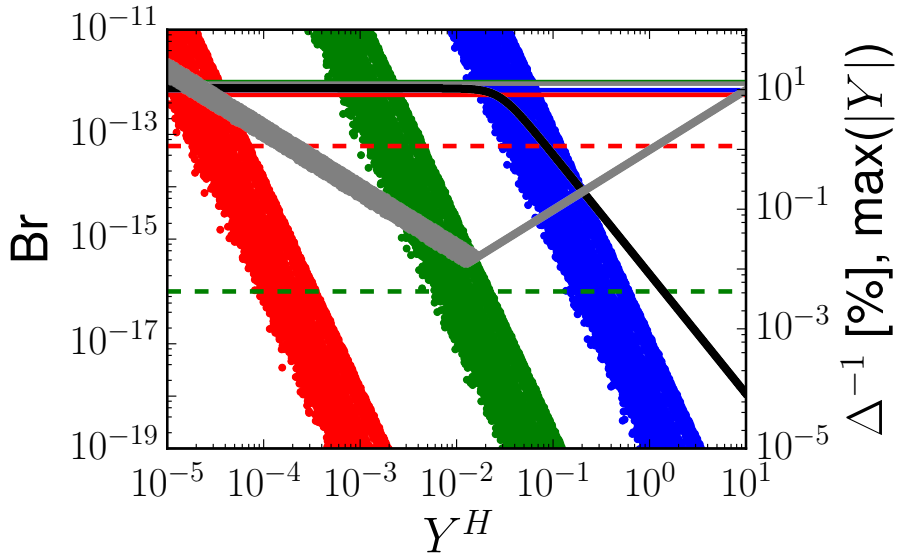


Figure 8: Same as Fig. 7. However the leptonic mixing parameters and neutrino mass squared differences are varied within the allowed 3σ ranges.

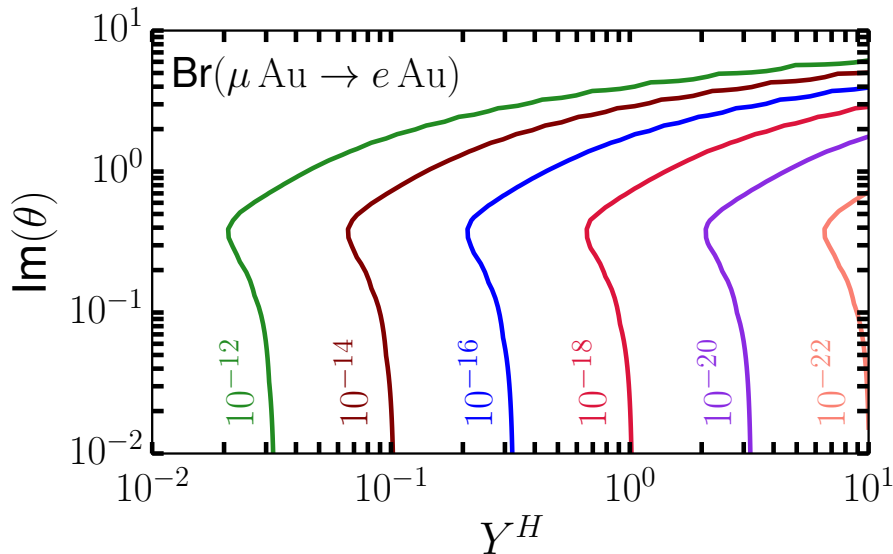


Figure 9: The contour lines show the branching ratio of μ - e conversion in gold calculated using meson exchange mediation as a function of the Yukawa coupling Y^H and the imaginary part of the angle θ parameterizing \mathcal{O} .

different colors and line styles are chosen in the same way as in Fig. 7. Fixing everything but the leptonic mixing parameters and mass squared differences, there is an uncertainty of up to three orders of magnitude in the rates for the different processes. Fig. 9 shows a contour plot of $\text{Br}(\mu\text{Au} \rightarrow e\text{Au})$ in the plane of the imaginary part of the complex angle θ in the complex orthogonal matrix \mathcal{O} and the Yukawa coupling Y^H . All LFV rates are relatively insensitive to the real part of θ and change at most at the percent level. A large imaginary part however leads to large Yukawa couplings Y^L canceling among each other to accommodate the light neutrino mass.

Finally we want to comment on the renormalization group evolution of the couplings in this model. The large $\text{SU}(2)$ representations lead to a strong running of the gauge couplings resulting in a Landau pole at a scale of about 10^9 GeV, where we have taken two-loop running into account. Similarly the quartic couplings of large scalar $\text{SU}(2)$ representations suffer from the triviality bound [73–75], because gauge couplings will induce these couplings at one-loop order, which will be further amplified by the running of the respective quartic coupling itself [75]. In particular, the study in Ref. [75] finds that the quartic coupling of the real quintuplet suffers from a Landau pole below 10^{15} GeV. A viable UV completion has to preserve the accidental Z_2 symmetry to prevent the minimal dark matter candidate from decaying. We are agnostic about the UV completion and mainly concentrate on phenomenology, since there are good prospects to ultimately test minimal dark matter models in the near future.

7 Conclusion

Embedding radiative neutrino mass models in the framework of MDM to make one theory work for two major fields of physics beyond the SM is aesthetically appealing. We systematically studied the possibility to realize this idea with radiative neutrino mass models as UV completions of the Weinberg operator. None of the minimal UV completions at one-loop leads to a stable minimal dark matter candidate. However we argued that it is feasible to obtain a cosmologically stable

dark matter candidate, because the decay is controlled by a coupling unrelated to neutrino mass generation, which can naturally be arbitrarily small.

We studied the phenomenology of one model explicitly. The model contains two real quintuplet scalars and also a quintuplet fermion whose neutral component field plays the role of dark matter. Both fields have zero hypercharge. In addition, a vector-like quadruplet fermion are introduced with hypercharge $\pm\frac{1}{2}$. We discussed the neutrino mass generation in this model and performed a detailed phenomenological study of lepton flavour violation and Higgs decay. There is a sizable allowed region of parameter space consistent with all current experimental constraints from Higgs physics and lepton flavor changing processes. The most stringent bound is placed by μ - e conversion in nuclei and will be further improved by future experiments. It places a lower bound on the Yukawa coupling Y^H and thus increases the electroweak fine-tuning. Current bounds already require at least $\sim 10\%$ tuning. In the near future, the remaining parameter space of this model can be tested by direct detection experiments like XENON 1T and indirect detection experiments such as CTA.

Acknowledgments

We thank Diego Aristizabal Sierra for pointing out the loop-induced decay modes of the minimal dark matter candidates via private communication and for useful discussions. We acknowledge the use of `matplotlib` [76] and `ipython` [77]. This work was supported in part by the Australian Research Council.

A Mass Matrix Diagonalization

The mass mixing in this model is proportional to $Y^H v/m_{\psi,\chi}$ and thus very suppressed for heavy masses of $\mathcal{O}(10)$ TeV. Although it can be safely neglected in most of the calculation as we did, we show the technical details for the diagonalization of the mass matrices for completeness.

The mass matrix for the neutral fermions can be diagonalised using a Takagi factorization, $V_0^* M_0 V_0^\dagger = M_0^D$. At leading order we find

$$M_0^D = \begin{pmatrix} m_\psi & & \\ & m_\psi & \\ & & m_\chi \end{pmatrix}, \quad V_0 = \begin{pmatrix} -\frac{i}{\sqrt{2}} & \frac{i}{\sqrt{2}} & \frac{ivY^H}{2\sqrt{2}(m_\chi+m_\psi)} \\ \frac{1}{\sqrt{2}} & \frac{1}{\sqrt{2}} & -\frac{vY^H}{\sqrt{2}(2m_\chi-2m_\psi)} \\ \frac{vY^H m_\chi}{2m_\chi^2-2m_\psi^2} & \frac{vY^H m_\psi}{2m_\chi^2-2m_\psi^2} & 1 \end{pmatrix}. \quad (44)$$

For the singly-charged fermions, the mass matrix M_1 can be diagonalised with a singular value decomposition $V_1^* X_1 W_1^\dagger = X_1^D$ with a diagonal matrix X_1^D and two unitary matrices V_1, W_1 . To the leading order they are given by

$$X_1^D = \begin{pmatrix} m_\psi & & \\ & m_\psi & \\ & & m_\chi \end{pmatrix}, \quad V_1 = \begin{pmatrix} \frac{1}{\sqrt{2}} & -\frac{1}{\sqrt{2}} & \frac{vY^H(\sqrt{3}m_\chi+m_\psi)}{4(m_\chi^2-m_\psi^2)} \\ -\frac{i}{\sqrt{2}} & -\frac{i}{\sqrt{2}} & -\frac{ivY^H(\sqrt{3}m_\chi-m_\psi)}{4(m_\chi^2-m_\psi^2)} \\ -\frac{\sqrt{\frac{3}{2}}vY^H m_\chi}{2m_\chi^2-2m_\psi^2} & \frac{vY^H m_\psi}{\sqrt{2}(2m_\chi^2-2m_\psi^2)} & 1 \end{pmatrix}, \quad (45)$$

$$W_1 = \begin{pmatrix} \frac{1}{\sqrt{2}} & -\frac{1}{\sqrt{2}} & \frac{vY^H(m_\chi+\sqrt{3}m_\psi)}{4(m_\chi^2-m_\psi^2)} \\ -\frac{i}{\sqrt{2}} & -\frac{i}{\sqrt{2}} & -\frac{ivY^H(m_\chi-\sqrt{3}m_\psi)}{4(m_\chi^2-m_\psi^2)} \\ -\frac{vY^H m_\chi}{\sqrt{2}(2m_\chi^2-2m_\psi^2)} & \frac{\sqrt{\frac{3}{2}}vY^H m_\psi}{2m_\chi^2-2m_\psi^2} & 1 \end{pmatrix}. \quad (46)$$

Similarly for the doubly-charged fermions, the mass matrix M_2 can be diagonalised with a singular value decomposition $V_2^* X_2 W_2^\dagger = X_2^D$ with a diagonal matrix X_2^D and two unitary matrices V_2, W_2 . To leading order they are given by

$$X_2^D = \begin{pmatrix} m_\psi & \\ & m_\chi \end{pmatrix}, \quad (47)$$

$$V_2 = \begin{pmatrix} 1 & -\frac{vY^H m_\chi}{\sqrt{2}(m_\chi^2 - m_\psi^2)} \\ \frac{vY^H m_\chi}{\sqrt{2}(m_\chi^2 - m_\psi^2)} & 1 \end{pmatrix}, \quad W_2 = \begin{pmatrix} 1 & \frac{vY^H m_\psi}{\sqrt{2}(m_\psi^2 - m_\chi^2)} \\ \frac{vY^H m_\psi}{\sqrt{2}(m_\chi^2 - m_\psi^2)} & 1 \end{pmatrix}. \quad (48)$$

B $SU(2)_L$ generators and the kinetic terms

All the odd-dimensional representations are real and even-dimensional representations pseudo-real. The generators of the four-dimensional representations can be explicitly written as

$$J_1^4 = \begin{pmatrix} 0 & -\frac{\sqrt{3}}{2} & 0 & 0 \\ -\frac{\sqrt{3}}{2} & 0 & -1 & 0 \\ 0 & -1 & 0 & \frac{\sqrt{3}}{2} \\ 0 & 0 & \frac{\sqrt{3}}{2} & 0 \end{pmatrix}, \quad J_2^4 = i \begin{pmatrix} 0 & \frac{\sqrt{3}}{2} & 0 & 0 \\ -\frac{\sqrt{3}}{2} & 0 & 1 & 0 \\ 0 & -1 & 0 & -\frac{\sqrt{3}}{2} \\ 0 & 0 & \frac{\sqrt{3}}{2} & 0 \end{pmatrix}, \quad (49)$$

$$J_3^4 = \text{diag}\left(\frac{3}{2}, \frac{1}{2}, -\frac{1}{2}, -\frac{3}{2}\right)$$

and the generators of the five-dimensional representation are given by

$$J_1^5 = \begin{pmatrix} 0 & -1 & 0 & 0 & 0 \\ -1 & 0 & -\sqrt{\frac{3}{2}} & 0 & 0 \\ 0 & -\sqrt{\frac{3}{2}} & 0 & \sqrt{\frac{3}{2}} & 0 \\ 0 & 0 & \sqrt{\frac{3}{2}} & 0 & 1 \\ 0 & 0 & 0 & 1 & 0 \end{pmatrix}, \quad J_2^5 = i \begin{pmatrix} 0 & 1 & 0 & 0 & 0 \\ -1 & 0 & \sqrt{\frac{3}{2}} & 0 & 0 \\ 0 & -\sqrt{\frac{3}{2}} & 0 & -\sqrt{\frac{3}{2}} & 0 \\ 0 & 0 & \sqrt{\frac{3}{2}} & 0 & -1 \\ 0 & 0 & 0 & 1 & 0 \end{pmatrix}, \quad (50)$$

$$J_3^5 = \text{diag}(2, 1, 0, -1, -2).$$

The kinetic terms for the exotic field are expressed as

$$\begin{aligned} \mathcal{L}^{kin} &= \frac{1}{2} (D_\mu \phi)^\dagger D^\mu \phi + i \chi^\dagger \bar{\sigma}^\mu D_\mu \chi + i \psi^\dagger \bar{\sigma}^\mu D_\mu \psi + i \bar{\psi}^\dagger \bar{\sigma}^\mu D_\mu \bar{\psi} \\ &\quad - \frac{1}{2} m_\phi^2 \phi^\dagger \phi - \frac{1}{2} m_\chi (\chi \chi + \chi^\dagger \chi^\dagger) - m_\psi (\psi \bar{\psi} + \psi^\dagger \bar{\psi}^\dagger) \\ &= (D_\mu \phi)^\dagger D^\mu \phi + i \chi_i^\dagger \bar{\sigma}^\mu D_\mu \chi_i + i \psi^\dagger \bar{\sigma}^\mu D_\mu \psi + i \bar{\psi}^\dagger \bar{\sigma}^\mu D_\mu \bar{\psi} \\ &\quad - m_\phi^2 \left(\frac{1}{2} \phi_0^2 + \phi^+ \phi^- + \phi^{++} \phi^{--} \right) \\ &\quad - m_\chi \left(\frac{1}{2} \chi^0 \chi^0 - \chi^- \chi^+ + \chi^{--} \chi^{++} + h.c. \right) \\ &\quad - m_\psi (\psi^0 \bar{\psi}^0 - \psi^+ \bar{\psi}^- - \psi^- \bar{\psi}^+ + \psi^{++} \bar{\psi}^{--} + h.c.), \end{aligned} \quad (51)$$

where the covariant derivatives are $D_\mu = \partial_\mu - ig J_a W_\mu^a - ig' Y B_\mu$.

References

- [1] M. Cirelli, N. Fornengo and A. Strumia, *Minimal dark matter*, *Nucl.Phys.* **B753** (2006) 178–194, [hep-ph/0512090].

- [2] M. Cirelli and A. Strumia, *Minimal Dark Matter: Model and results*, *New J. Phys.* **11** (2009) 105005, [0903.3381].
- [3] E. Del Nobile, M. Nardecchia and P. Panci, *Millicharge or Decay: A Critical Take on Minimal Dark Matter*, 1512.05353.
- [4] S. Dodelson and L. M. Widrow, *Sterile-neutrinos as dark matter*, *Phys. Rev. Lett.* **72** (1994) 17–20, [hep-ph/9303287].
- [5] L. M. Krauss, S. Nasri and M. Trodden, *A Model for neutrino masses and dark matter*, *Phys. Rev.* **D67** (2003) 085002, [hep-ph/0210389].
- [6] E. Ma, *Verifiable radiative seesaw mechanism of neutrino mass and dark matter*, *Phys. Rev.* **D73** (2006) 077301, [hep-ph/0601225].
- [7] L. Basso, O. Fischer and J. J. van der Bij, *Natural Z model with an inverse seesaw mechanism and leptonic dark matter*, *Phys. Rev.* **D87** (2013) 035015, [1207.3250].
- [8] S. S. C. Law and K. L. McDonald, *A Class of Inert N-tuplet Models with Radiative Neutrino Mass and Dark Matter*, *JHEP* **09** (2013) 092, [1305.6467].
- [9] A. Ahriche, C.-S. Chen, K. L. McDonald and S. Nasri, *Three-loop model of neutrino mass with dark matter*, *Phys. Rev.* **D90** (2014) 015024, [1404.2696].
- [10] P. Minkowski, $\mu \rightarrow e\gamma$ at a rate of one out of 1-billion muon decays?, *Phys. Lett.* **B67** (1977) 421.
- [11] T. Yanagida, *Horizontal gauge symmetry and masses of neutrinos*, in *Proceedings of the Workshop on The Unified Theory and the Baryon Number in the Universe* (O. Sawada and A. Sugamoto, eds.), p. 95, KEK, Tsukuba, Japan, 1979.
- [12] S. L. Glashow, *The future of elementary particle physics*, in *Proceedings of the 1979 Cargèse Summer Institute on Quarks and Leptons* (M. L. vy, J.-L. Basdevant, D. Speiser, J. Weyers, R. Gastmans and M. Jacob, eds.), pp. 687–713, Plenum Press, New York, 1980.
- [13] M. Gell-Mann, P. Ramond and R. Slansky, *Complex spinors and unified theories*, in *Supergravity* (P. van Nieuwenhuizen and D. Z. Freedman, eds.), p. 315, North Holland, Amsterdam, 1979.
- [14] R. N. Mohapatra and G. Senjanović, *Neutrino mass and spontaneous parity violation*, *Phys. Rev. Lett.* **44** (1980) 912.
- [15] M. Magg and C. Wetterich, *Neutrino mass problem and gauge hierarchy*, *Phys. Lett.* **B94** (1980) 61.
- [16] J. Schechter and J. Valle, *Neutrino Masses in SU(2) x U(1) Theories*, *Phys.Rev.* **D22** (1980) 2227.
- [17] C. Wetterich, *Neutrino masses and the scale of B – L violation*, *Nucl. Phys.* **B187** (1981) 343.
- [18] G. Lazarides, Q. Shafi and C. Wetterich, *Proton lifetime and fermion masses in an SO(10) model*, *Nucl. Phys.* **B181** (1981) 287.
- [19] R. N. Mohapatra and G. Senjanovic, *Neutrino Masses and Mixings in Gauge Models with Spontaneous Parity Violation*, *Phys.Rev.* **D23** (1981) 165.

- [20] T. Cheng and L.-F. Li, *Neutrino Masses, Mixings and Oscillations in $SU(2) \times U(1)$ Models of Electroweak Interactions*, *Phys.Rev.* **D22** (1980) 2860.
- [21] R. Foot, H. Lew, X. He and G. C. Joshi, *Seesaw neutrino masses induced by a triplet of leptons*, *Z.Phys.* **C44** (1989) 441.
- [22] A. Zee, *A Theory of Lepton Number Violation, Neutrino Majorana Mass, and Oscillation*, *Phys. Lett.* **B93** (1980) 389.
- [23] Y. Cai, X.-G. He, M. Ramsey-Musolf and L.-H. Tsai, *$R\nu$ MDM and Lepton Flavor Violation*, *JHEP* **12** (2011) 054, [1108.0969].
- [24] K. Kumericki, I. Picek and B. Radovcic, *Critique of Fermionic $R\nu$ MDM and its Scalar Variants*, *JHEP* **07** (2012) 039, [1204.6597].
- [25] A. Ahriche, K. L. McDonald and S. Nasri, *A Model of Radiative Neutrino Mass: with or without Dark Matter*, *JHEP* **10** (2014) 167, [1404.5917].
- [26] P. Culjak, K. Kumericki and I. Picek, *Scotogenic $R\nu$ MDM at three-loop level*, *Phys. Lett.* **B744** (2015) 237–243, [1502.07887].
- [27] A. Ahriche, K. L. McDonald, S. Nasri and T. Toma, *A Model of Neutrino Mass and Dark Matter with an Accidental Symmetry*, *Phys. Lett.* **B746** (2015) 430–435, [1504.05755].
- [28] K. Kumericki, I. Picek and B. Radovcic, *TeV-scale Seesaw with Quintuplet Fermions*, *Phys. Rev.* **D86** (2012) 013006, [1204.6599].
- [29] F. Bonnet, M. Hirsch, T. Ota and W. Winter, *Systematic study of the $d=5$ Weinberg operator at one-loop order*, *JHEP* **07** (2012) 153, [1204.5862].
- [30] D. A. Sierra, C. Simoes and D. Wegman, *Closing in on minimal dark matter and radiative neutrino masses*, 1603.04723.
- [31] A. Ahriche, K. L. McDonald, S. Nasri and I. Picek, *Radiative neutrino mass via both minimal dark matter candidates*, 1603.01247.
- [32] G. 't Hooft, *Naturalness, chiral symmetry, and spontaneous chiral symmetry breaking*, *NATO Sci. Ser. B* **59** (1980) 135.
- [33] A. Ibarra, A. S. Lamperstorfer and J. Silk, *Dark matter annihilations and decays after the AMS-02 positron measurements*, *Phys. Rev.* **D89** (2014) 063539, [1309.2570].
- [34] C. Rott, K. Kohri and S. C. Park, *Superheavy dark matter and IceCube neutrino signals: Bounds on decaying dark matter*, *Phys. Rev.* **D92** (2015) 023529, [1408.4575].
- [35] S. Ando and K. Ishiwata, *Constraints on decaying dark matter from the extragalactic gamma-ray background*, *JCAP* **1505** (2015) 024, [1502.02007].
- [36] G. Giesen, M. Boudaud, Y. Gnolini, V. Poulin, M. Cirelli, P. Salati et al., *AMS-02 antiprotons, at last! Secondary astrophysical component and immediate implications for Dark Matter*, *JCAP* **1509** (2015) 023, [1504.04276].
- [37] PLANCK collaboration, P. A. R. Ade et al., *Planck 2015 results. XIII. Cosmological parameters*, 1502.01589.
- [38] M. Cirelli, T. Hambye, P. Panci, F. Sala and M. Taoso, *Gamma ray tests of Minimal Dark Matter*, *JCAP* **1510** (2015) 026, [1507.05519].

- [39] J. Casas and A. Ibarra, *Oscillating neutrinos and $\mu \rightarrow e\gamma$* , *Nucl.Phys.* **B618** (2001) 171–204, [[hep-ph/0103065](#)].
- [40] N. D. Christensen and C. Duhr, *FeynRules - Feynman rules made easy*, *Comput.Phys.Commun.* **180** (2009) 1614–1641, [[0806.4194](#)].
- [41] T. Hahn, *Generating Feynman diagrams and amplitudes with FeynArts 3*, *Comput.Phys.Commun.* **140** (2001) 418–431, [[hep-ph/0012260](#)].
- [42] T. Hahn and M. Perez-Victoria, *Automatized one loop calculations in four-dimensions and D-dimensions*, *Comput.Phys.Commun.* **118** (1999) 153–165, [[hep-ph/9807565](#)].
- [43] P. W. Angel, Y. Cai, N. L. Rodd, M. A. Schmidt and R. R. Volkas, *Testable two-loop radiative neutrino mass model based on an $LLQd^cQd^c$ effective operator*, *JHEP* **10** (2013) 118, [[1308.0463](#)].
- [44] PARTICLE DATA GROUP collaboration, K. A. Olive et al., *Review of Particle Physics*, *Chin. Phys.* **C38** (2014) 090001.
- [45] *Projections for measurements of Higgs boson cross sections, branching ratios and coupling parameters with the ATLAS detector at a HL-LHC*, Tech. Rep. ATL-PHYS-PUB-2013-014, CERN, Geneva, Oct, 2013.
- [46] L. Lavoura, *General formulae for $f_1 \rightarrow f_2\gamma$* , *Eur. Phys. J.* **C29** (2003) 191–195, [[hep-ph/0302221](#)].
- [47] MEG collaboration, J. Adam et al., *New constraint on the existence of the $\mu^+ \rightarrow e^+\gamma$ decay*, *Phys. Rev. Lett.* **110** (2013) 201801, [[1303.0754](#)].
- [48] A. M. Baldini et al., *MEG Upgrade Proposal*, [1301.7225](#).
- [49] MUON G-2 collaboration, G. W. Bennett et al., *Final Report of the Muon E821 Anomalous Magnetic Moment Measurement at BNL*, *Phys. Rev.* **D73** (2006) 072003, [[hep-ex/0602035](#)].
- [50] J. Hisano, T. Moroi, K. Tobe and M. Yamaguchi, *Lepton flavor violation via right-handed neutrino Yukawa couplings in supersymmetric standard model*, *Phys. Rev.* **D53** (1996) 2442–2459, [[hep-ph/9510309](#)].
- [51] J. Hisano and D. Nomura, *Solar and atmospheric neutrino oscillations and lepton flavor violation in supersymmetric models with the right-handed neutrinos*, *Phys. Rev.* **D59** (1999) 116005, [[hep-ph/9810479](#)].
- [52] E. Arganda and M. J. Herrero, *Testing supersymmetry with lepton flavor violating tau and mu decays*, *Phys. Rev.* **D73** (2006) 055003, [[hep-ph/0510405](#)].
- [53] SINDRUM collaboration, U. Bellgardt et al., *Search for the Decay $\mu^+ \rightarrow e^+e^+e^-$* , *Nucl. Phys.* **B299** (1988) 1.
- [54] A. Blondel et al., *Research Proposal for an Experiment to Search for the Decay $\mu \rightarrow eee$* , [1301.6113](#).
- [55] R. Kitano, M. Koike and Y. Okada, *Detailed calculation of lepton flavor violating muon electron conversion rate for various nuclei*, *Phys. Rev.* **D66** (2002) 096002, [[hep-ph/0203110](#)].
- [56] COMET collaboration, E. V. Hungerford, *COMET/PRISM muon to electron conversion at J-PARC*, *AIP Conf. Proc.* **1182** (2009) 694–697.

- [57] COMET collaboration, Y. G. Cui et al., *Conceptual design report for experimental search for lepton flavor violating $\mu^- e^-$ conversion at sensitivity of 10^{*-16} with a slow-extracted bunched proton beam (COMET)*, .
- [58] MU2E collaboration, R. M. Carey et al., *Proposal to search for $\mu^- N \rightarrow e^- N$ with a single event sensitivity below 10^{-16}* , .
- [59] COMET collaboration, A. Kurup, *The COherent Muon to Electron Transition (COMET) experiment*, *Nucl. Phys. Proc. Suppl.* **218** (2011) 38–43.
- [60] R. K. Kutschke, *The Mu2e Experiment at Fermilab*, in *Proceedings, 31st International Conference on Physics in collisions (PIC 2011)*, 2011. 1112.0242.
- [61] LUX collaboration, D. S. Akerib et al., *First results from the LUX dark matter experiment at the Sanford Underground Research Facility*, *Phys. Rev. Lett.* **112** (2014) 091303, [1310.8214].
- [62] Y. Cai and A. P. Spray, *Fermionic Semi-Annihilating Dark Matter*, *JHEP* **01** (2016) 087, [1509.08481].
- [63] XENON collaboration, E. Aprile et al., *Physics reach of the XENON1T dark matter experiment*, *Submitted to: JCAP* (2015) , [1512.07501].
- [64] K. Bernloehr et al., *The optical system of the HESS imaging atmospheric Cherenkov telescopes, Part 1: Layout and components of the system*, *Astropart. Phys.* **20** (2003) 111–128, [astro-ph/0308246].
- [65] CTA CONSORTIUM collaboration, M. Actis et al., *Design concepts for the Cherenkov Telescope Array CTA: An advanced facility for ground-based high-energy gamma-ray astronomy*, *Exper. Astron.* **32** (2011) 193–316, [1008.3703].
- [66] B. Ostdiek, *Constraining the minimal dark matter fiveplet with LHC searches*, *Phys. Rev. D* **92** (2015) 055008, [1506.03445].
- [67] C. Garcia-Cely, A. Ibarra, A. S. Lamperstorfer and M. H. G. Tytgat, *Gamma-rays from Heavy Minimal Dark Matter*, *JCAP* **1510** (2015) 058, [1507.05536].
- [68] M. Cirelli, F. Sala and M. Taoso, *Wino-like Minimal Dark Matter and future colliders*, *JHEP* **10** (2014) 033, [1407.7058].
- [69] M. Low and L.-T. Wang, *Neutralino dark matter at 14 TeV and 100 TeV*, *JHEP* **08** (2014) 161, [1404.0682].
- [70] M. C. Gonzalez-Garcia, M. Maltoni and T. Schwetz, *Updated fit to three neutrino mixing: status of leptonic CP violation*, *JHEP* **11** (2014) 052, [1409.5439].
- [71] SINDRUM II collaboration, C. Dohmen et al., *Test of lepton flavor conservation in $\mu \rightarrow e$ conversion on titanium*, *Phys. Lett.* **B317** (1993) 631–636.
- [72] SINDRUM II collaboration, W. H. Bertl et al., *A Search for muon to electron conversion in muonic gold*, *Eur. Phys. J.* **C47** (2006) 337–346.
- [73] N. Cabibbo, L. Maiani, G. Parisi and R. Petronzio, *Bounds on the fermions and higgs boson masses in grand unified theories*, *Nucl. Phys.* **B158** (1979) 295.
- [74] M. Lindner, *Implications of triviality for the standard model*, *Zeitschrift für Physik C Particles and Fields* **31** (1986) 295–300.

- [75] Y. Hamada, K. Kawana and K. Tsumura, *Landau pole in the Standard Model with weakly interacting scalar fields*, 1505.01721.
- [76] J. D. Hunter, *Matplotlib: A 2d graphics environment*, *Computing in Science and Engineering* **9** (2007) 90–95.
- [77] F. Pérez and B. E. Granger, *IPython: a system for interactive scientific computing*, *Computing in Science and Engineering* **9** (May, 2007) 21–29.